Anlotininb as a Promising Inhibitor on Tumor Growth of Oral Squamous Cell Carcinoma Through Cell Apoptosis and Mitotic Catastrophe

Zhaoming Deng
Fifth Affiliated Hospital of Sun Yat-sen University https://orcid.org/0000-0001-9013-6013
Wei Liao
Fifth Affiliated Hospital of Sun Yat-sen University
Wei Wei
Fifth Affiliated Hospital of Sun Yat-sen University
Guihua Zhong
Fifth Affiliated Hospital of Sun Yat-sen University
Chao He
Fifth Affiliated Hospital of Sun Yat-sen University
Hongbo Zhang
Fifth Affiliated Hospital of Sun Yat-sen University
Qiaodan Liu
Fifth Affiliated Hospital of Sun Yat-sen University
Xiwei Xu
Fifth Affiliated Hospital of Sun Yat-sen University
Jun Liang (liangjun@mail.sysu.edu.cn)
The Fifth Affiliated Hospital of Sun Yat-sen University, Zhuhai https://orcid.org/0000-0002-5866-9239
Zhigang Liu
Fifth Affiliated Hospital of Sun Yat-sen University

Primary research

Keywords: Oral squamous cell carcinoma, Anlotinib, VEGFR-2, Cell Apoptosis, Cell cycle arrest, Mitotic catastrophe

Posted Date: October 6th, 2020

DOI: https://doi.org/10.21203/rs.3.rs-80678/v1

Version of Record: A version of this preprint was published on January 9th, 2021. See the published version at https://doi.org/10.1186/s12935-020-01721-x.

Abstract

Background

Oral squamous cell carcinoma (OSCC) has been one of the most malignant cancers in head and neck region. Anlotinib is a tyrosine kinase inhibitor targeting several receptors such as vascular endothelial growth factor receptor (VEGFR), fibroblast growth factor receptor (FGFR), platelet-derived growth factor receptor (PDGFR) and c-Kit. Here we investigated whether Anlotinib have any antitumor effect on oral cancer and tried to explore and explain the possible mechanism.

Methods

Data from The Cancer Genome Atlas and the Gene Expression Omnibus and Gene Expression Omnibus database was collected to analyze the relationship between the expression of vascular epithelial growth factor receptor 2 and the overall survival rate of OSCC. Oral cancer cell lines Cal-27 and SCC-25 were cultured to conduct all the experiments. In vitro experiments such as CCK-8, colony formation, cell cycle assay and cell apoptosis assay were conducted to detect cell proliferation ability and the change of cell phase and apoptosis. Proteins concerning cell cycle and cell apoptosis were visualized via western blot. α-Tubulin were visualized via immunofluorescence to detect cells undergoing mitotic catastrophe.

Results

Higher expression of VEGFR-2 was significantly related to poorer prognosis. Experiment in vitro demonstrated that cell proliferation was significantly inhibited($p<0.05$) after Anlotinib administration and G2/M arrest and apoptosis were both detected in both cell lines. Cycle-related proteins promoting cell cycle progression and proteins related to cell survival were downregulated in Anlotinib group compared to the control group. Cell-death-related biomarker and phosphorylated histone 3 were upregulated in expression in Anlotinib group. Abnormal spindle apparatus was observed in cells undergoing mitotic catastrophe.

Conclusion

Anlotinib could exert an antitumor effect on oral cancer cells lines via apoptotic pathway and mitotic catastrophe pattern, presenting a promising potential therapy for patients with OSCC.

Background

Oral squamous cell carcinoma (OSCC) has been one of the most malignant cancers in the head and neck region. Incidence of OSCC is rising globally especially in regions or countries with heavy tobacco-consumption and alcohol abuse. Males could be affected by OSCC more often than females for much more frequent exposure to tobacco and alcoholic drinking[1]. In India, however, females present higher risks of intraoral carcinoma because of heavier indulgence of tobacco chewing behavior[2,3]. It is reported that the incidence of the OSCC in recent decades is showing a significant climbing in young

subjects of western world. Unfortunately, survival rate has not improved obviously in patients of OSCC whose primary treatment is the surgical intervention and chemotherapy if indicating metastasis of the cancer.

Anlotinib is a tyrosine kinase inhibitor targeting several receptors such as vascular endothelial growth factor receptor (VEGFR), fibroblast growth factor receptor (FGFR), platelet-derived growth factor receptor (PDGFR) and c-Kit. There are researches showing that Anlotinib has obvious antitumorigenic effect in several cancer such as thyroid cancer, soft tissue sarcoma and metastatic colorectal cancer[4-6]. In a phase-3 randomized clinical trial covering 439 patients with advanced non-small cell lung cancer, Anlotinib provided a prolonged overall survival rate and progression-free survival rate[7]. However, there is little research looking into the efficacy of administration of Anlotinib on patients with OSCC. Here we investigated in vitro and in vivo whether Anlotinib have any antitumor effect on oral cancer and tried to explore and explain the possible mechanism.

Materials And Methods

3.1 Cell Lines Culture

Human oral squamous cell lines Cal-27 and SCC-25 were obtained from Genechem Co, Ltd (Genechem, Shanghai, China) and cultured carefully in RPMI 1640 Medium(Cal-27) and DMEM/F12(1:1) (SCC-25) (Thermo Fisher Scientific, MA, USA) consisting of 10% fetal bovine serum (FBS) (Thermo Fisher Scientific, MA, USA) and 1% penicillin/streptomycin (Thermo Fisher Scientific, MA, USA. All Cell cultures were maintained at 37 Celsius with 5% CO_2 in a humidified incubator before the following in vitro experiments.

3.2 The Cancer Genome Atlas (TCGA) and the Gene Expression Omnibus (GEO) Data

Data from TCGA (https://tcga-data.nci.nih.gov/tcga/) and GEO (https://www.ncbi.nlm.nih.gov/geo/) was downloaded and collected to analyze the relationship between the prognosis of head and neck squamous cell carcinoma (HNSC) and VEGFR-2 expression.

3.3 Cell Proliferation Viability Assay

Cell counting kit 8 (CCK-8) (MedChemExpress, USA) was adopted to examine the cell proliferation viability. Cells were seeded in a 96-well plate with a density of 2,000 cells per well. To find out an optimal toxicity effect on the cancer cells, Anlotinib with various concentration was added 24 hours after cell seeding in the plate of each cell lines before CCK-8 (1:10 diluted in 100μL medium per well) was added in each plate 24,48 and 72 hours later. After incubation of the mixture for 3 hours, measurement of Formazan generated was carried out at 450 nm using a microplate reader (Molecular Devices CMax Plus, USA). Relative percentage of cell survival was counted by dividing the absorbance value of treated cells by that of the control group in each cell lines.

3.4 Cell Cycle and Cell Apoptotic Assay

Cells were incubated with or without Anlotinib for 24 hours and harvested before staining with Propidium iodide (PI, BD Biosciences, USA). To detect apoptotic percentage, cells of different groups were harvested to be stained with FITC (BD Biosciences, USA) and Annexin-V (BD Biossciences, USA) before the flow cytometry analysis (DeFlex, Beckman Coulter, Inc.USA). Data from cell cycle was transformed to graphs with the help of ModFit LT3.0 (VerifySoftware House, Topsham, ME, USA) while apoptotic data was visualized via FlowJo V10.0(BD Biosciences, USA).

3.5 Colony Formation Assay

Cells were seeded in 6-well plates at a density of 300 cells per well. 24 hours later, the medium was replaced by fresh one with Anlotinib of the optimal concentration resulted from CCK-8 Assay while medium of control group was replaced without any change in constitution. After another 24 hours of incubation together, medium of both groups was removed to be added with fresh Anlotinib-free medium, followed by 14-day incubation during which medium was freshened on a regular basis. At the end of the assay, colonies were visible enough to be fixed with 4% Paraformaldehyde (Bioss, Beijing, China) for 15 minutes and another 15-minute staining with crystal violet (Sigma Life Science), after which the results were all processed with the help of ImageJ.

3.6 Western Blotting

Western blotting was performed as previously described. Antibodies was used to detect protein such as cdc2(#9116, 1:1000, CST), phospho-cdc2(#4539, 1:1000, CST), Chk2(#6334, 1:1000, CST), phospho-Chk2(#2197, 1:1000, CST), CyclinB1(#12231, 1:1000,CST), Bax(#5023, 1:1000, CST), Bcl-2(#15071, 1:1000, CST), Caspase-3(#14220, 1:1000, CST), Cleaved Caspase-3(#9664, 1:1000, CST), PARP(#9532, 1:1000, CST), Cleaved PARP(#5625, 1:1000, CST), phosphor-Histone H3(#53348, 1:1000, CST) and α-tubulin(#2125, 1:1000,CST). β-Actin was chosen as internal control. Signal was visualized via Supersignal Western Blot Enhancer (#46640, Thermo Fisher Scientific, USA) using a Chemiluminescent Imaging System (Tanon, Shanghai, China)

3.7 Immunofluorescence assay

Immunofluorescence assay was performed in a 24-well plate for cell line Cal-27. Cells were harvested and fixed with 4% paraformaldehyde and permeated with 0.3% Triton X-100. After blocking with 5% BSA (Bovine Serum Albumin), cells were incubated overnight at 4℃ with primary antibodiesα-tubulin(#2125, 1:25,CST). Fluorophore-conjugated secondary antibodies (#4414, 1:400, CST) were used to incubate the specimens at room temperature for 1 hour. DAPI was used to stain the nuclear of the cells in the final step. Specimens were finally observed and images were captured under an immunofluorescence microscope. All of the steps were operated in the dark after adding Fluorophore-conjugated secondary antibodies.

3.8 Statistical Analysis

All the data collected was analyzed by SPSS 17.0 (SPSS, Inc., Chicago, IL, USA). Survival curves were drawn using Kapplan-Meier method. Log-rank test was adopted to compare high and low expression groups for VEGFR-2. Two- tailed P value less than 0.05 was defined as statistically significant.

Results

4.1 Poor prognosis was related to higher expression of VEGFR-2

As VEGFR-2 was the major target of Anlotinib[8], data covering 517 specimens (259 high expression and 258 low expression) from TCGA demonstrated that poor prognosis was significantly related to higher expression of VEGFR-2 ($p<0.05$) (Figure 1A). Data concerning 93 samples from the Gene Expression Omnibus presented a slight relationship between the overall survival rate and high expression of VEGFR-2 ($p=0.07$) (Figure 1B). Expression was found to be significantly higher in tumoral tissues than in the adjacent normal tissues ($p<0.05$) (Figure 1C).

Figure 1. Data from TCGA and GEO databases were collected to analyze the relationship between prognosis and the expression of VEGFR-2. TCGA data concerning 517 specimens showed poor prognosis were closely related to high expression of VEGFR-2 ($p<0.05$) (A) while data from GEO demonstrated slight relationship ($p=0.07$) (B). Higher expression of mRNA was found in tumoral tissues($n=42$) than in adjacent normal tissues ($n=499$) when analyzing data from TCGA database (C). (*$p<0.05$, **$p<0.01$)

4.2 Anlotinib suppressed short and long-term proliferation viability of oral cancer cell lines

The results of CCK-8 assay demonstrated that cell proliferation in short term of oral cancer cell lines (Cal-27 and SCC-25) was significantly suppressed by Anlotinib with a dose-dependent pattern ($p<0.01$) (Figure 2A, B). Colony formation was performed for each cell line to find that long-term cell proliferation was greatly inhibited by Anlotinib compared to the control group ($p<0.01$). (Figure 2C, D)

Figure 2. Anlotinib inhibited cell viability of proliferation. Three consecutive days of CCK-8 test showed Anlotinib suppressed cell proliferation in a dose-dependent pattern (A, B). Colony formation confirmed the inhibitive effect of Anlotinib.(C, D) (*$p<0.05$, **$p<0.01$)

4.3 Cell cycle arrest and cell apoptosis were induced by Anlotinib

G1/S and G2/M arrest were detected in cell line Cal-27 treated with Anlotinib. ($P<0.01$) (Figure 3A, B) while G2/M arrest was observed in SCC-25 treated with Anlotinib. ($P< 0.01$) (Figure 3C, D). Compared to the control group, cell apoptosis, including early apoptosis and general apoptosis, was induced in both cell lines treated with Anlotinib. ($P< 0.05$) (Figure 3E~G).

Figure 3. Cell cycle arrest and cell apoptosis were induced by Anlotinib. Cells were treated with Anlotinib for 24 hours before harvest for flow cytometry to detect cell cycle distribution, and for 48 hours to detect cell apoptotic percentage. The results demonstrated cell cycle percentage of G2 was significantly raised from 8.94% (Cal-27) and 15.21% (SCC-25) to 12.66% and 30.25% (A-D). Cell apoptotic percentage (early

apoptosis and total apoptosis) was significantly increased in groups treated with Anlotinib (E-H). (*p<0.05, **p<0.01)

4.4 Down-regulated expression of VEGFR-2 was induced by Anlotinib

Western blot was conducted to find that the expression of VEGFR-2 was decreased in both cell lines treated by Anlotinib in a dose-dependent pattern (Figure 4A).

4.5 Cell Cycle procedure was interrupted by Anlotinib

Marker concerning cell cycle procedure, including cdc-2, phosphorylated cdc-2, Chk-2, phosphorylated Chk-2 and Cyclin B1, was detected via western blot in expression (Figure 4B). Obviously, expression of phosphorylated cdc-2 and Chk-2 was downregulated in both cell lines after Anlotinib administration. Cyclin B1 was also decreased in expression. Phosphorylated histone 3 was detected to increase in expression.

4.6 Cell death was induced by the way of cell apoptosis with change in expression of related proteins.

Survival-related biomarker Bcl-2 was detected to be inhibited while proteins concerning cell apoptosis such as Bax, Caspase-3(non or phosphorylated) and PAPR (non or phosphorylated) were all visualized to be upregulated after Anlotinib treatment. (Figure 4C)

Figure 4. Expression of VEGFR2, cell-cycle-related and apoptosis-related protein was visualized by western blot. Anlotinib inhibited the expression of VEGFR2 on cell line Cal-27 and SCC-25 (A). Key checkpoint biomarkers such as phosphorylated-Chk-2, phosphorylated-Cdc-2 and Cyclin B1 was down-regulated after Anlotininb administration. Phosphorylated histone 3 was upregulated in anlotinib-treated group (B). Expression of such apoptotic biomarkers as Bax, Cleaved-Caspase-3 and Cleaved-PARP increased in Anlotinib-treated groups. Bcl-2 was downregulated in expression. (C).

4.7 Nuclear instability and abnormal mitosis were induced as a result of Anlotinib administration

Abnormal spindle apparatus labeled with α-Tubulin was captured in Anlotinib group of Cal-27, which was characterized with tetraploid and poly-central mitosis. (Figure 5A). Higher percentage of nuclear breakage was found in Anlotinib group than control group (Figure 5B).

Figure5. Nucleus chromosome instability and mitotic catastrophe were observed and visualized in Cal-27 via immunofluorescence. Normal mitosis was presented in a bipolar pattern of spindles apparatus by α-Tubulin-labeled staining of immunofluorescence while in Anlotinib-treated group, spindles in cells were not heading to two but four poles or even more (A). Significant nuclear breakage was found in Anlotinib-treated group (20.1%) than in control group (5.4%) (B) (*p<0.05, **p<0.01).

Discussion

As a multitargeting tyrosine inhibitor in clinical development, Anlotinib exerts antitumor effects through anti-angiogenesis activity targeting multiple tyrosine kinases such as vascular endothelial growth factor receptor 1/2/3 (VEGFR-1/2/3), platelet-derived growth factor receptor (PDGFR) and fibroblast growth factor receptor (FGFR)[8]. It was reported that Anlotinib have significant antitumoral effect on solid tumor including thyroid cancer[9], non-small lung cancer[10], soft tissue sarcoma[11], renal cancer[12] and gastric cancer[13]. However, there is little research focusing on whether Anlotinib have an antitumor effect on oral squamous cell carcinoma which is one of the most common cancers in head and neck region.

Cell death was considered to include several forms such as apoptosis (Programmed cell death), necrosis (Uncontrolled cell death), autophagy, ferroptosis, oncosis, pyroptosis and mitotic failure[14,15]. Distinct biomarkers could be detected to determine which pathway of death cells are going through. Mitotic catastrophe is a one of the cell death pathways that characterizes several abnormal cellular biological processes such as defect of nuclear division, multinucleation or micronucleation, which could be a result of factors including DNA damage, abnormal checkpoint of cell cycle especially the M phase and spindle apparatus, microtubes poisoning, overheat and presence of tetraploid. A healthy G2/M transformation is greatly dependent on an undisrupted progress of the combination of cyclin-dependent kinase 1 (CDK-1) and cyclin B1 which guarantees multiple important nuclear activities such as the condensation of chromosome, breakdown of nuclear membrane during mitosis and remodeling of microtubes[16]. Anaphase-promoting complex (APC), a key driver of the degradation of cyclin B and securin during middle-late phase, the end of mitosis, could negatively disturb normal progression of cell cycle and induce mitotic failure by prolonging activation period of CDK-1 as a result of a consistent self-inhibition.

In our work, we found a downregulation of phosphorylated cdc-2 (p-cdc-2), an important biomarker pushing cells to enter cell cycle[17], and a decreasing Cyclin B1 after Anlotinib administration, which significantly block the normal transformation of a cell trying to start up mitosis. Failure of combination of p-cdc-2 and Cyclin B1 during the late stage of cell cycle is a depending factor to induce G2/M arrest. Blockage of cell cycle along with generation of apoptotic signals disrupted microtubes condensation and chromosome instability. Histone within nuclear plays a key role in regulating gene expression[18]. Different kind of modification of histone have different effect on gene regulation. Generally, phosphorylated form of histone could bother the normal tie with DNA which consequently destabilize the chromosome and disturb the remodeling and condensing of homologous chromosome during mitosis[18]. In our work, an upregulated expression of phosphorylated Histone 3 was detected via western blot and immunofluorescence, indicating cells were undergoing chromosome disturbance. α-Tubulin was visualized to monitor the contour of spindles apparatus in mitotic cell via immunofluorescence. Unlike healthy mitosis, abnormal spindles were observed in cells after Anlotinib administration, characterizing the presence of tetraploid or even multipolar spindles which doomed a death for a cell.

Conclusions

Within the limitation of the research, Anlotinib exerted an antitumor effect on oral squamous cell carcinoma cell lines (Ca-27 and SCC-25) by inducing cell death via cell apoptosis and cell cycle arrest.

Disorder of cycle checkpoints combined with generation of apoptotic signals might be a reason to induce abnormal mitosis. Failure of condensation of spindle apparatus was a key driver to induce mitotic catastrophe, rendering chromosome instability and a nuclear or cell configuration far from normal pattern. Significant antitumor effect was observed in vivo and vitro experiments, indicating that Anlotinib might have a potential curable effect on patients with OSCC with a hopeful efficacy.

Abbreviations

OSCC: Oral squamous cell carcinoma

VEGFR: vascular endothelial growth factor receptor

FGFR: Fibroblast growth factor receptor

PDGFR: platelet-derived growth factor receptor

CCK-8: Cell counting kit-8

TCGA: The Cancer Genome Atlas

GEO: The Gene Expression Omnibus

HNSC: head and neck squamous cell carcinoma

Cdk-1: cyclin-dependent kinase 1

APC: Anaphase-promoting complex

Declarations

Ethics approval and consent to participate

Not applicable

Consent for publication

Not applicable

Availability of data and materials

All data generated or analyzed during this study are included in this published article and its additional files.

Competing interests

The authors declare that they have no competing interests

Funding

This study was funded by Beijing Medical and Health Public Welfare Fund (Grant No. F3040C) and The Fundamental Research Funds for the Central Universities (Grant No.19ykzd07).

Acknowledgements

Not applicable

Author Contributions

Conceptualization, Jun Liang and Zhigang Liu; Data curation, Chao He; Formal analysis, Chao He; Investigation, Wei Wei and Hongbo Zhang; Methodology, Zhaoming Deng and Xiwei Xu; Project administration, Jun Liang; Resources, Guihua Zhong; Software, Wei Liao; Supervision, Jun Liang and Zhigang Liu; Validation, Hongbo Zhang; Visualization, Qiaodan Liu; Writing – original draft, Zhaoming Deng; Writing – review & editing, Wei Liao and Wei Wei.

References

1. Hill, S.J.; D'Andrea, A.D. Predictive Potential of Head and Neck Squamous Cell Carcinoma Organoids. *Cancer Discov* **2019**, *9*, 828-830, doi:10.1158/2159-8290.CD-19-0527.
2. D'Souza, G.; Robbins, H.A. Sexual and relationship health among survivors of oropharyngeal or oral cavity squamous cell carcinoma. *Cancer* **2017**, *123*, 1092-1094.
3. Gupta, B.; Bray, F.; Kumar, N.; Johnson, N.W. Associations between oral hygiene habits, diet, tobacco and alcohol and risk of oral cancer: A case-control study from India. *Cancer Epidemiol* **2017**, *51*, 7-14, doi:10.1016/j.canep.2017.09.003.
4. Ruan, X.; Shi, X.; Dong, Q.; Yu, Y.; Hou, X.; Song, X.; Wei, X.; Chen, L.; Gao, M. Antitumor effects of anlotinib in thyroid cancer. *Endocr Relat Cancer* **2019**, *26*, 153-164, doi:10.1530/ERC-17-0558.
5. Chi, Y.; Fang, Z.; Hong, X.; Yao, Y.; Sun, P.; Wang, G.; Du, F.; Sun, Y.; Wu, Q.; Qu, G., et al. Safety and Efficacy of Anlotinib, a Multikinase Angiogenesis Inhibitor, in Patients with Refractory Metastatic Soft-Tissue Sarcoma. *Clin Cancer Res* **2018**, *24*, 5233-5238, doi:10.1158/1078-0432.Ccr-17-3766.
6. Li, N.; Huang, Q.; Zhang, M.J.; Chen, Z.D. [Efficacy and safety of Anlotinib as a third-line chemotherapy for metastatic colorectal cancer]. *Zhonghua Yi Xue Za Zhi* **2019**, *99*, 2844-2847, doi:10.3760/cma.j.issn.0376-2491.2019.36.010.
7. Han, B.; Li, K.; Wang, Q.; Zhang, L.; Shi, J.; Wang, Z.; Cheng, Y.; He, J.; Shi, Y.; Zhao, Y., et al. Effect of Anlotinib as a Third-Line or Further Treatment on Overall Survival of Patients With Advanced Non-Small Cell Lung Cancer: The ALTER 0303 Phase 3 Randomized Clinical Trial. *JAMA Oncol* **2018**, *4*, 1569-1575, doi:10.1001/jamaoncol.2018.3039.
8. Shen, G.; Zheng, F.; Ren, D.; Du, F.; Dong, Q.; Wang, Z.; Zhao, F.; Ahmad, R.; Zhao, J. Anlotinib: a novel multi-targeting tyrosine kinase inhibitor in clinical development. *J Hematol Oncol* **2018**, *11*, 120, doi:10.1186/s13045-018-0664-7.

9. Sun, Y.; Du, F.; Gao, M.; Ji, Q.; Li, Z.; Zhang, Y.; Guo, Z.; Wang, J.; Chen, X.; Wang, J., et al. Anlotinib for the Treatment of Patients with Locally Advanced or Metastatic Medullary Thyroid Cancer. *Thyroid* **2018**, *28*, 1455-1461, doi:10.1089/thy.2018.0022.
10. Yang, X.; Xiang, M.; Geng, L.; Wen, Y.; Du, X. Anlotinib Combined with S-1 in the Third-Line Treatment of Stage IV Non-Small Cell Lung Cancer: Study Protocol for Phase II Clinical Trial. *Asian Pac J Cancer Prev* **2019**, *20*, 3849-3853, doi:10.31557/APJCP.2019.20.12.3849.
11. Wang, Z.M.; Zhang, S.L.; Yang, H.; Zhuang, R.Y.; Guo, X.; Tong, H.X.; Zhang, Y.; Lu, W.Q.; Zhou, Y.H. Efficacy and safety of anlotinib, a multikinase angiogenesis inhibitor, in combination with epirubicin in preclinical models of soft tissue sarcoma. *Cancer Med* **2020**, 10.1002/cam4.2941, doi:10.1002/cam4.2941.
12. Ma, J.; Song, Y.; Shou, J.; Bai, Y.; Li, H.; Xie, X.; Luo, H.; Ren, X.; Liu, J.; Ye, D., et al. Anlotinib for Patients With Metastatic Renal Cell Carcinoma Previously Treated With One Vascular Endothelial Growth Factor Receptor-Tyrosine Kinase Inhibitor: A Phase 2 Trial. *Front Oncol* **2020**, *10*, 664, doi:10.3389/fonc.2020.00664.
13. Wang, J.; Wu, D.X.; Meng, L.; Ji, G. Anlotinib combined with SOX regimen (S1 (tegafur, gimeracil and oteracil porassium capsules) + oxaliplatin) in treating stage IV gastric cancer: study protocol for a single-armed and single-centred clinical trial. *BMJ Open* **2020**, *10*, e034685, doi:10.1136/bmjopen-2019-034685.
14. Majno, G.; Joris, I. Apoptosis, oncosis, and necrosis. An overview of cell death. *Am J Pathol* **1995**, *146*, 3-15.
15. D'Arcy, M.S. Cell death: a review of the major forms of apoptosis, necrosis and autophagy. *Cell Biol Int* **2019**, *43*, 582-592, doi:10.1002/cbin.11137.
16. Rieder, C.L. Mitosis in vertebrates: the G2/M and M/A transitions and their associated checkpoints. *Chromosome Res* **2011**, *19*, 291-306, doi:10.1007/s10577-010-9178-z.
17. Huang, T.S.; Shu, C.H.; Chao, Y.; Chen, S.N.; Chen, L.L. Activation of MAD 2 checkprotein and persistence of cyclin B1/CDC 2 activity associate with paclitaxel-induced apoptosis in human nasopharyngeal carcinoma cells. *Apoptosis* **2000**, *5*, 235-241, doi:10.1023/a:1009652412399.
18. Stillman, B. Histone Modifications: Insights into Their Influence on Gene Expression. *Cell* **2018**, *175*, 6-9, doi:10.1016/j.cell.2018.08.032.

Figures

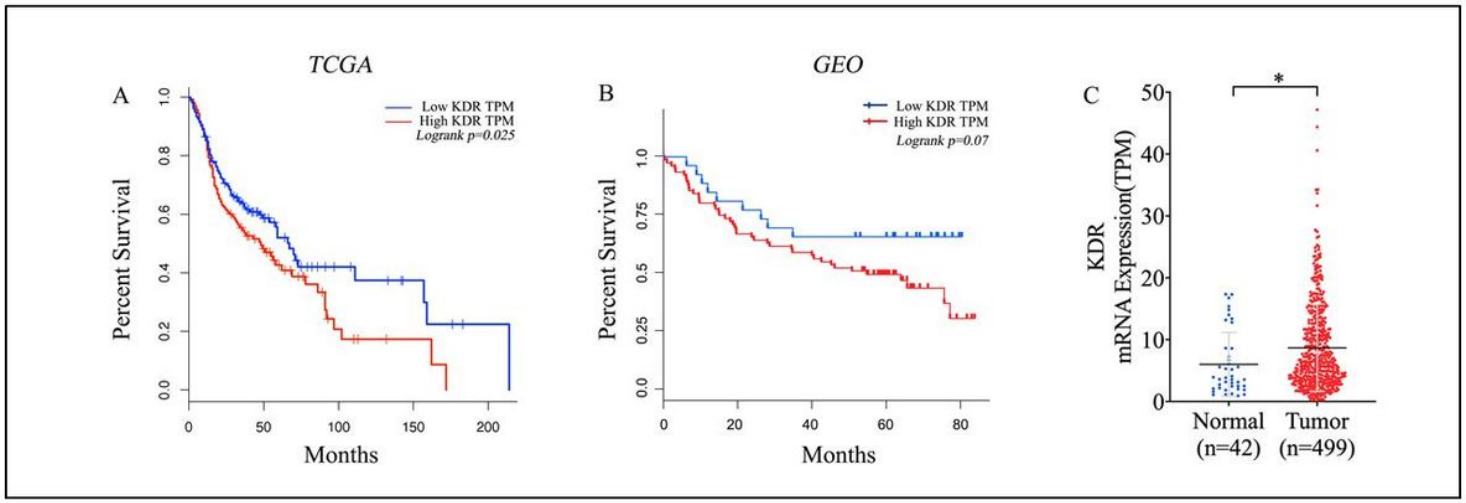

Figure 1

Data from TCGA and GEO databases were collected to analyze the relationship between prognosis and the expression of VEGFR-2. TCGA data concerning 517 specimens showed poor prognosis were closely related to high expression of VEGFR-2 ($p<0.05$) (A) while data from GEO demonstrated slight relationship ($p=0.07$) (B). Higher expression of mRNA was found in tumoral tissues(n=42) than in adjacent normal tissues (n=499) when analyzing data from TCGA database (C). (*$p<0.05$, **$p<0.01$)

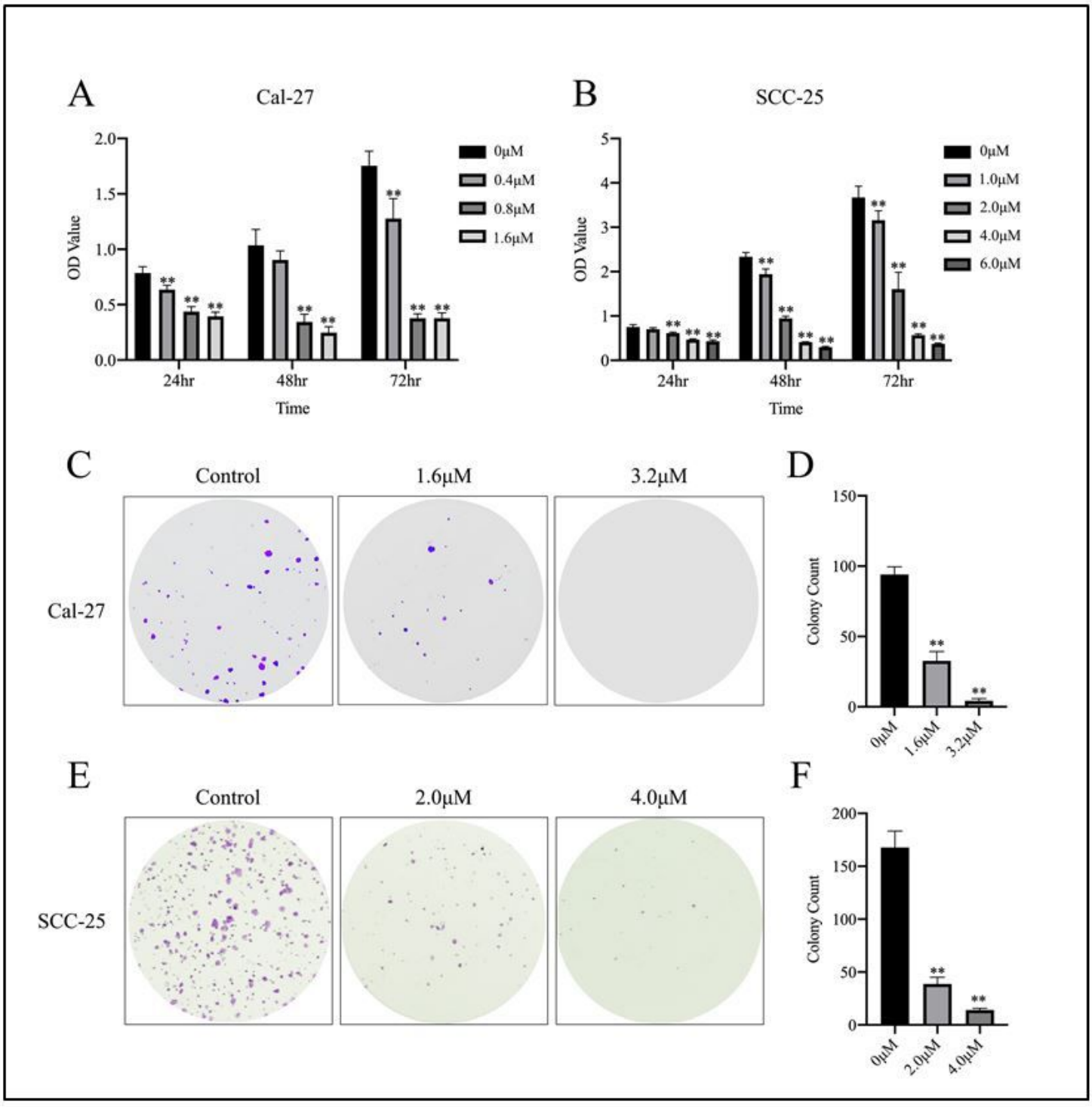

Figure 2

Anlotinib inhibited cell viability of proliferation. Three consecutive days of CCK-8 test showed Anlotinib suppressed cell proliferation in a dose-dependent pattern (A, B). Colony formation confirmed the inhibitive effect of Anlotinib.(C, D) (*p<0.05, **p<0.01)

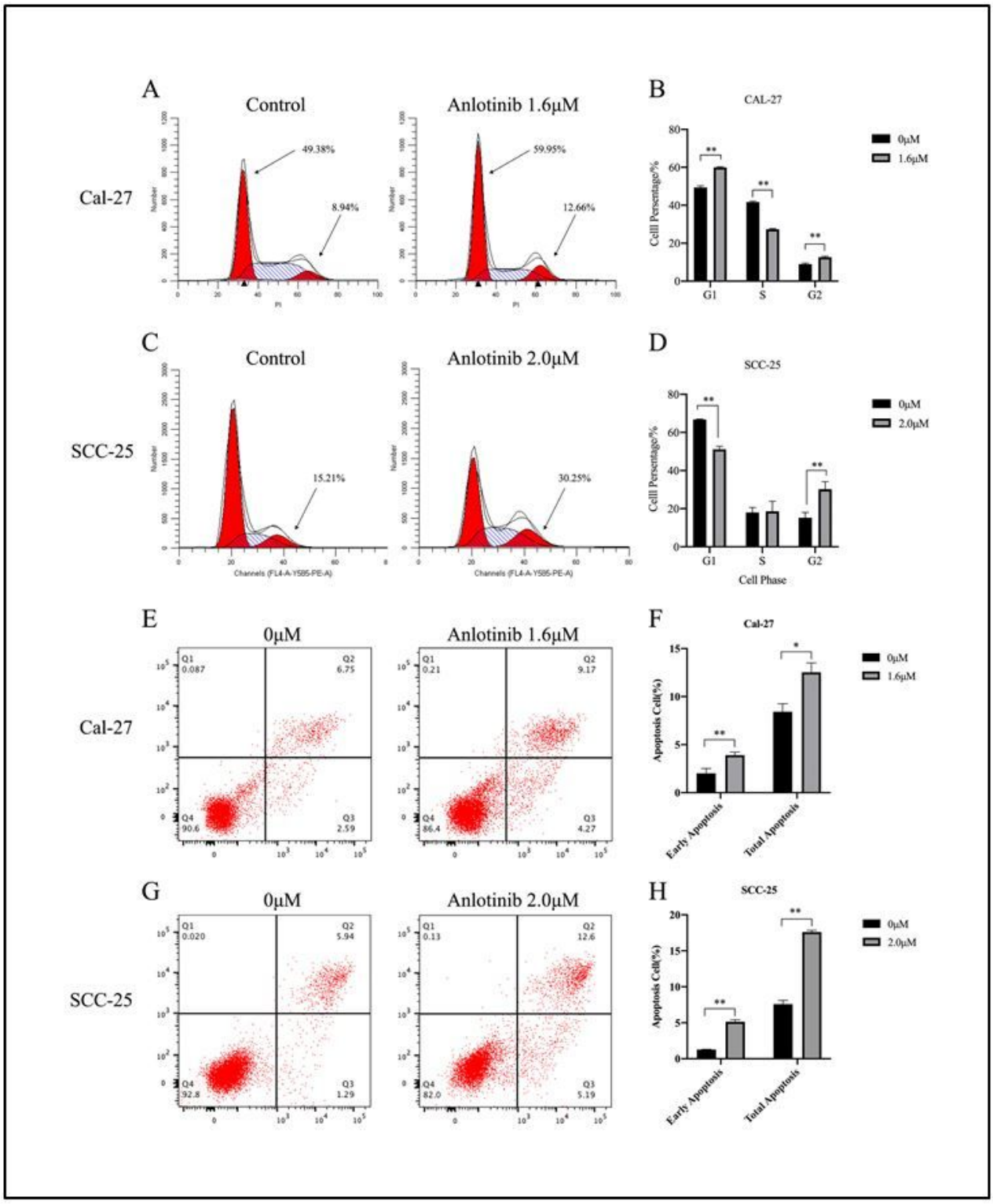

Figure 3

Cell cycle arrest and cell apoptosis were induced by Anlotinib. Cells were treated with Anlotinib for 24 hours before harvest for flow cytometry to detect cell cycle distribution, and for 48 hours to detect cell apoptotic percentage. The results demonstrated cell cycle percentage of G2 was significantly raised from 8.94% (Cal-27) and 15.21% (SCC-25) to 12.66% and 30.25% (A-D). Cell apoptotic percentage (early

apoptosis and total apoptosis) was significantly increased in groups treated with Anlotinib (E-H). (*p<0.05, **p<0.01)

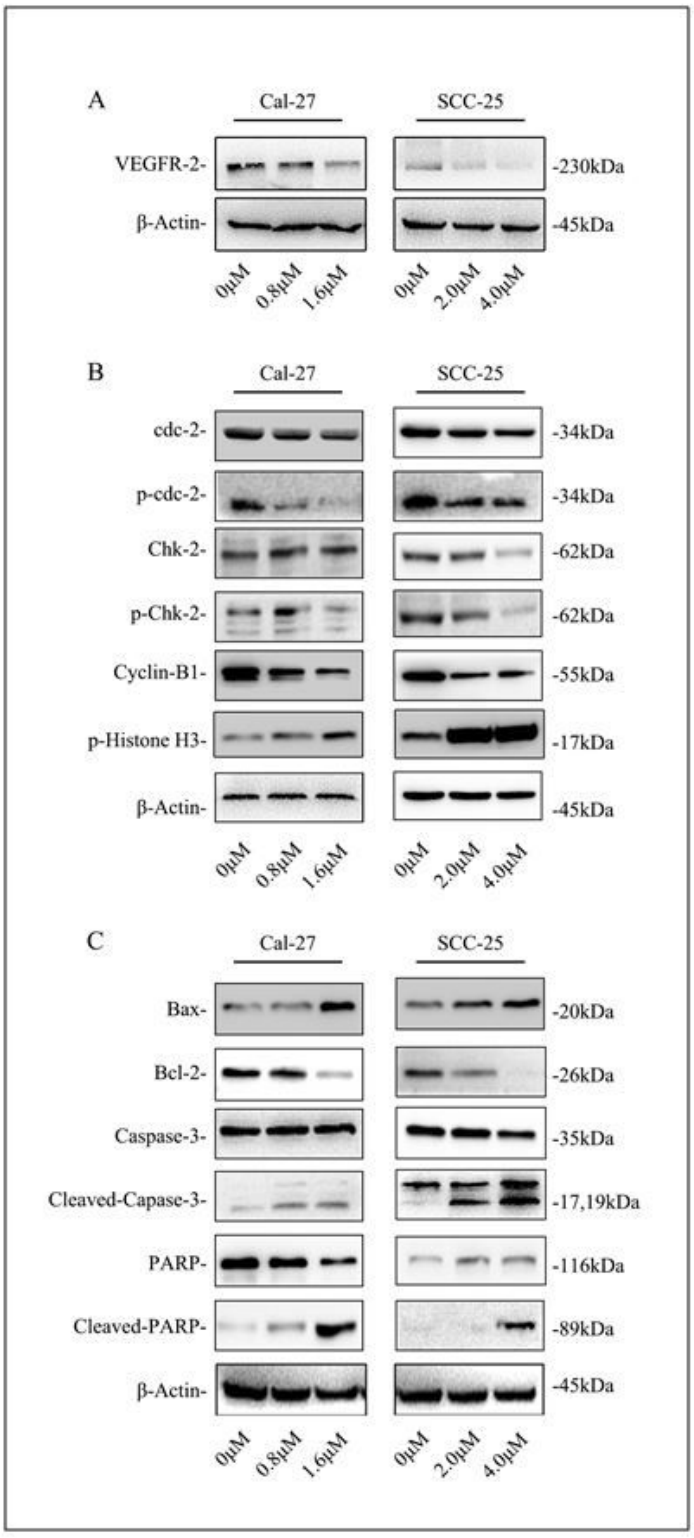

Figure 4

Expression of VEGFR2, cell-cycle-related and apoptosis-related protein was visualized by western blot. Anlotinib inhibited the expression of VEGFR2 on cell line Cal-27 and SCC-25 (A). Key checkpoint biomarkers such as phosphorylated-Chk-2, phosphorylated-Cdc-2 and Cyclin B1 was down-regulated after

Anlotininb administration. Phosphorylated histone 3 was upregulated in anlotinib-treated group (B). Expression of such apoptotic biomarkers as Bax, Cleaved-Caspase-3 and Cleaved-PARP increased in Anlotinib-treated groups. Bcl-2 was downregulated in expression. (C).

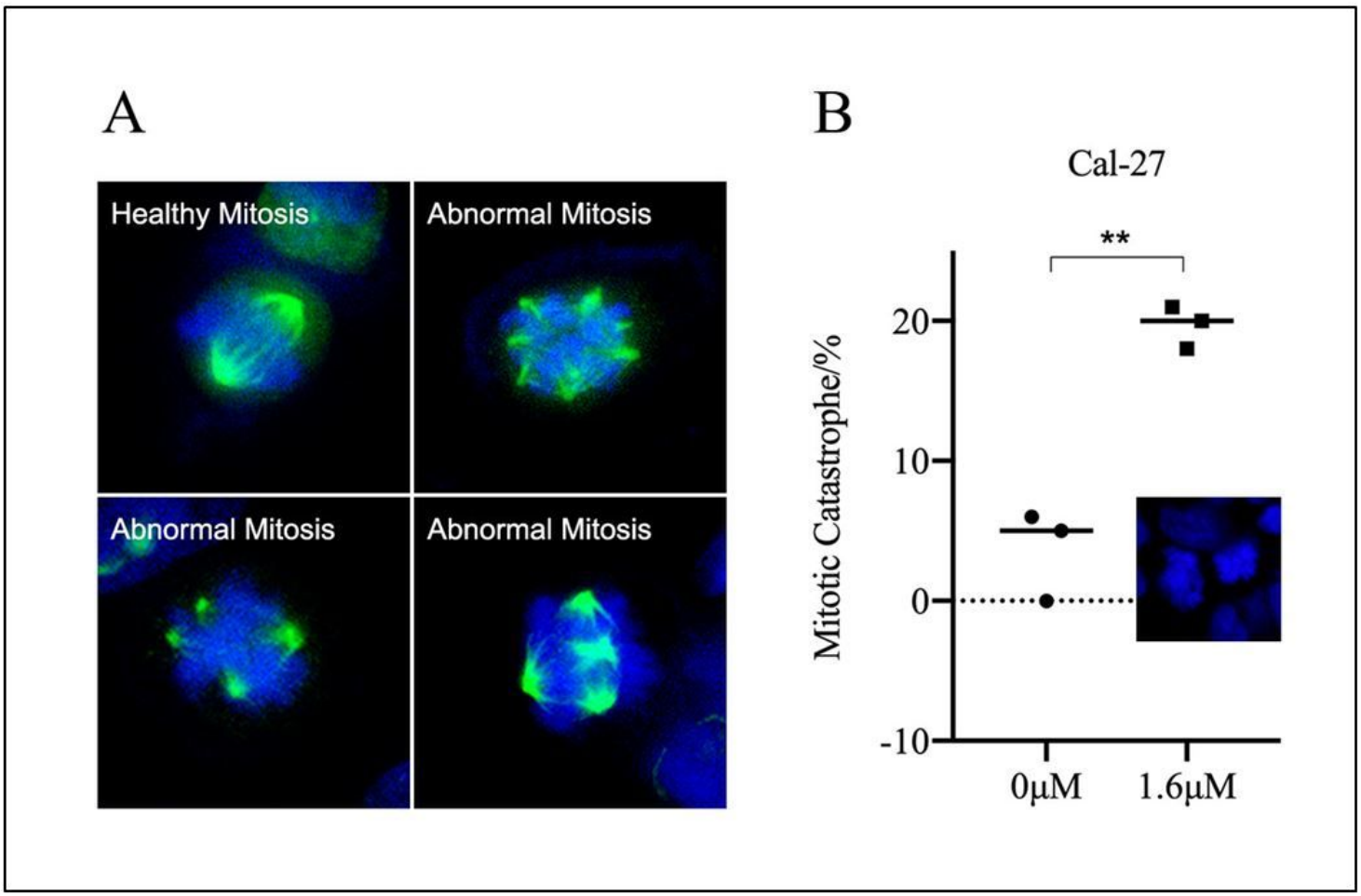

Figure 5

Nucleus chromosome instability and mitotic catastrophe were observed and visualized in Cal-27 via immunofluorescence. Normal mitosis was presented in a bipolar pattern of spindles apparatus by α-Tubulin-labeled staining of immunofluorescence while in Anlotinib-treated group, spindles in cells were not heading to two but four poles or even more (A). Significant nuclear breakage was found in Anlotinib-treated group (20.1%) than in control group (5.4%) (B) (*p<0.05, **p<0.01).